Chapter 2

INSTRUMENTS/TECHNIQUES USED FOR CHARACTERIZATION OF SYNTHESIZED MATERIALS

The synthesized compounds organic ammonium chloride salts (OACSs), organic-inorganic hybrid compounds (OIHCs) and organic ammonium nitrate salts (OANSs) were characterized by various techniques such as Fourier Transform Infrared Spectroscopy (FT-IR), Elemental Analyzer (CHN), Nuclear Magnetic Resonance (NMR), X-Ray Diffraction (XRD), Thermal Analysis [Thermogravimetry/Differential Thermal Analyzer (TG/DTA), Differential Scanning Calorimetry (DSC)], Raman Spectroscopy, Electron Paramagnetic Resonance (EPR), Scanning Electron Microscope (SEM) and Mercury Porosimeter, Superconducting Quantum Interference Device (SQUID) measurement. This chapter will outline theory behind these experimental techniques.

2.1 Fourier Transform Infrared Spectroscopy (FT-IR)

Infrared spectrum is an important record which gives sufficient information about the functional group of the compound. Absorption in the infrared region is due to the change in the vibrational and rotational levels. The most important source of infrared light for scanning of spectrum of an organic compound is Nernst glower, which is consist of a rod of the sintered mixture of oxides of Zirconium, Ytterbium and Erbium. The rod is electrically heated to 1973 K to produce infrared radiation. A rod of silicon carbide (Globar) can also be electrically heated to produce infrared radiations. Infrared region of the spectrum is divided into three main sections.

1) Near infrared (overtone region): 13333 - 4000 cm^{-1}
2) Infrared (vibration-rotation region): 4000 - 400 cm^{-1}
3) Far infrared (rotation region): 400 - 10 cm^{-1}

The main region of infrared spectrum which is of greatest importance to chemist is infrared which lie between 4000 - 400 cm^{-1}. It was originally designed as a double beam spectrophotometer comprising infrared source, grating monochromator, thermocouple detector, cells etc. To obtained monochromic light, optical prisms or grating can be used. For prism material, glass or quartz cannot be used since they absorb strongly through most of infrared region. Sodium chloride (most usually) or of potassium bromide, silver chloride or cesium bromide are commonly used as cell containers or for prism materials as these are transparent to most of the infrared region

under consideration. In this process the light is dispersed by the monochromator. But, this type of basic design for infrared measurements has been outdated. In a newer technique termed FT-IR has been in practice. This technique utilizes a single beam of un-dispersed light and has the instrument components similar to the previous one. In FT-IR, the un-dispersed light beam is passed through the sample and the absorbance at all wavelengths are received at the detector simultaneously. A computerized mathematical manipulation (known as "Fourier Transform") is performed on this data, to obtain absorption data for each and every wavelength. To perform this type of calculations interference of light pattern is required for which the FT-IR instrumentation contains two mirrors, one fixed and one moveable with a beam splitter in between them. Before scanning the sample a reference or a blank scanning is required this is illustrated in Figure 2.1.

Figure 2.1 Fourier Transform Infrared Spectroscopy, Perkin Elmer Spectrum RX1 FT-IR.

Various techniques can be employed for placing the sample in the path of the infrared beam depending upon whether the sample is gas, liquid or solid. The spectra were obtained in infrared region using solid state technique. We were used Perkin Elmer Spectrum RX1 FT-IR instrument for obtained vibrational spectra. Samples were diluted with spectroscopic KBr and pressed into a pellet. Scanned were run over the range 4000 - 400 cm^{-1}. It will be immediately apparent that this spectrum may be divided into two parts, first between 4000 - 1600 cm^{-1} and second from 1600 - 660 cm^{-1}. The former are relatively few absorption bands termed the 'functional group region' but in the latter a great number of absorptions termed the 'fingerprint region' are observed.

2.2 Elemental Analyzer (CHN)

This technique determines the presence of the elements like Carbon, Hydrogen and Nitrogen in a given substance and gives the result as percentage amount of these atoms against the total weight. With a conversion kit Sulphur and Oxygen can be analyzed. Since this technique specifically determines these five elements this instrument is also called as "CHNS/O Analyzer".

The combustion train filled with oxygen and the sample is injected. Combustion occurs under static conditions in an excess of oxygen at about 1248 K. The products of combustion are passed over suitable reagents in the combustion tube to assure complete oxidation and removal of undesirable by-products such as sulfur, phosphorous and halogen gases. In the reduction tube, oxides of nitrogen are converted to molecular nitrogen and residual oxygen is removed. In the mixing volume the sample gasses are thoroughly homogenized at a precise volume, temperature and pressure. This mixture is released through sample volume into the thermal conductivity detector. Between the first of three pairs of thermal conductivity cells an absorption trap removes water from the sample gas. The differential signal read before and after the trap reflects the water concentration. Therefore, the amount of hydrogen retained in the original sample. A similar measurement is performed of the signal output of a second pair of thermal conductivity cells, between which a trap removes carbon dioxide, ultimately determined the carbon content. The remaining gas has helium and nitrogen only. This gas passed through a thermal conductivity cell and the output signal is compared to reference cell through which pure helium flows. This gives nitrogen concentration (Figure 2.2).

Furthermore, sulfur analysis carried out by the combustion tube replaced with tungstic oxide packing plus a dehydration reagent. The water trap is removed and replaced with silver oxide to absorb SO. The sample is handled and run as before, but the sulfur from the sample is oxidized to form SO_2, and the water formed is removed. The concentration of SO_2 is detected and measured likewise hydrogen analysis method.

Figure 2.2 Elemental Analyzer, Fisons EA1108.

For oxygen analysis, the combustion tube replaced by a pyrolysis tube composed of platinized carbon. The reduction tube is replaced by an oxidation tube containing copper oxide. The sample is handled and run as before, but is now pyrolyzed in presence of helium. So, in the sample, carbon monoxide is formed from oxygen. The CO is oxidized by the copper oxide to form carbon dioxide, which is detected and measured in the same manner as the carbon analysis.

For elemental analyses we were used Perkin Elmer, Series II, 2400. Sulphanilamide was taken as reference material.

2.3 Nuclear Magnetic Resonance (NMR)

NMR spectrophotometer makes use of a magnet, a radio-frequency, a detector and an amplifier. The detection system is used to note that energy is being transferred from the radio-frequency beam to the nucleus. The sample under investigation is taken in a glass tube which is placed between the pole faces of a magnet. A radio-frequency source (v = 400 mega cycles sec^{-1}) is made to fall on the sample. It can be done by feeding energy (Radio-frequency source) into a coil wound round the sample tube. A signal is detected if the nuclei in the sample resonate with the source, i.e. ΔE, energy required to flip the proton is the same as that of the source. Energy is transferred from the source via nuclei to the detector coil. The output from the

detector can be fed to a cathode ray oscillograph or to a strip chart recorder after amplication *etc*. NMR spectrum consists of series of peaks that correspond to different applied field strengths. Each peak means a set of protons.

NMR spectroscopy is a powerful tool for the chemist. This technique is only applicable to those nuclei which possess a spin quantum number (I) greater than zero. The most significant nuclei for the chemist concerned are ^{1}H and ^{13}C which have quantum number of ½. Moreover, the other nuclei with non-zero spin quantum numbers are ^{19}F and ^{31}P with $I = ½$; ^{14}N and ^{2}D, with $I = 1$ and ^{11}B and ^{35}Cl, with $I = ³/₂$. The nucleus of hydrogen atom (proton) behaves as a spinning bar magnet because it possesses both electric and magnetic spin. Likewise, other spinning charged body; the nucleus of hydrogen atom generates a magnetic field. NMR involves the interaction between an oscillating magnetic field of electromagnetic radiation and the magnetic energy of the hydrogen nucleus of some other type of nuclei when these are placed in an external static magnetic field. The sample absorbs electromagnetic radiation in radio wave region at different frequencies since absorption depends upon the type of protons or certain nuclei contained in the sample. When proton is placed in a magnetic field, then it starts precessing at a certain frequency in the radio wave region and thus, will be capable of taking up one of the two orientations with respect to the axis of the external field.

1) Alignment with the field
2) Alignment against the field

If proton is precessing in the aligned orientation, it can pass into the opposed orientation by absorbing energy. From the high energy opposed orientation, it comes back to the low energy aligned orientation (more stable) by losing energy. The transition from one energy state to the other is called flipping of the proton. The transition between the two energy states can be brought about by the absorption of a quantum of electromagnetic radiation in the radio wave with energy hv. The energy required to bring about the transition ($\Delta E = hv$) or to flip the proton depends upon the strength of the external field. The proton will precess at different frequencies. Now, these precessing protons with steadily changing frequencies (for promoting or flipping protons from the low energy state to high energy state) and observe

frequency/frequencies at which absorption occur. It is generally more convenient to keep the radio-frequency constant and the strength of the magnetic field is constantly varied. At some value of the field strength, the energy required to flip the protons matches the energy of the radiation. Absorption occurs and a signal is observed. Such a spectrum is called NMR spectrum. The photograph of NMR is shown in Figure 2.3.

Figure 2.3 NMR spectrophotometer.

When molecule placed in magnetic field, its electrons are caused to circulate and thus, they produce secondary magnetic fields i.e., induced magnetic field. Rotation of electrons about the proton itself generates a field that can either oppose or reinforce the applied field. If the induced field opposed the applied field, then proton is said to be shielded. But if the induced field reinforces the applied field, proton feels higher field strength and such proton is said to be deshielded. Such shifts in the positions of NMR due to shielding or deshielding of protons by the electrons are called chemical shift. For measuring the chemical shifts of various protons in the molecule, the signal of tetra methyl silane is taken as a reference. Due to the low electro negativity of silicon, the shielding of equivalent protons in tetramethylsilane (TMS) is greater than most of the organic compounds. In the NMR signal for particular proton in a molecule will appear at different field strengths compared to a signal from TMS. This difference in the absorption position of proton with respect to TMS signal is called chemical shift (δ-value). The valve of δ for the substance with respect to TMS can be define as

$$\delta = \frac{\nu_{sample} - \nu_{reference}}{\text{operating frequency in megacycles}}$$

$$= \frac{\Delta\nu}{\text{operating frequency in megacycles}}$$

Where $\Delta\nu$ = frequency shift. The value of δ is expressed in parts per million (ppm).

We were used Bruker Avance 400 MHz spectrometer for NMR spectra. Chemical shift are quoted using the δ scale, with $\delta = 0$ referenced to TMS. The solutions were prepared by dissolving 5 - 10 mg of compounds in dimethyl sulfoxide-d_6 (Fischer scientific, 99.9 atom% D, < 50 ppm water) solvent.

2.4 X-Ray Diffraction (XRD)

Single Crystal X-ray diffraction (XRD) has become a powerful tool for unambiguous and accurate determination of molecular structure and atomic spacing. Even though XRD by crystals and its use in determining crystal structure and many other properties of solid state. X-rays are produced when accelerated electrons (electrons with sufficient kinetic energy generated by heating a Tungsten filament) fall on a target. Usually targets are metals with sufficiently high melting points. The commonly used X-ray targets (anti-cathodes) for producing X-rays for diffraction studies are Cu, Mo, Au, Fe, Co, Ag etc. When electrons with sufficient kinetic energy impinge on the target it knocks out the electrons from the inner shells of the target atoms. Since the inner shells cannot remain vacant; electrons from higher orbits fall to the vacant shell radiating the difference of energy. Transitions from higher to lower shells have to follow the selection rules for angular momentum conservation. The rays produced due to electronic transition from L to K shell is called Kα line; the one from M to K shell is called Kβ line and N to K the Kγ line; the one from M to L is Lα line etc. Since each of the shells have many energy levels within themselves, the X-rays termed by Kα, Kβ, Kγ etc. are multiples, the most common is Kα and Kβ. The Kα consists, in part, of Kα_1 and Kα_2. Kα_1 has a slightly shorter wavelength and twice the intensity as Kα_2. The specific wavelengths are characteristic of the target material. Filtering, by foils or crystal monochrometers (Nb, Zr etc.), is required to produce monochromatic X-rays needed for diffraction. Kα_1 and Kα_2 are sufficiently close in wavelength such that a weighted average of the two is used. Molybdenum and copper

are the most common target materials for single crystal diffraction, with Mo Kα radiation = 0.7107 Å and Cu Kα radiation = 1.5418 Å.

These X-rays are generated by a cathode ray tube, filtered to produce monochromatic radiation, collimated to concentrate, and directed toward the sample. The interaction of the incident rays with the sample produces constructive interference (and a diffracted ray) when conditions satisfy Bragg's Law ($n\lambda=2d\sin\theta$). This law relates the wavelength of electromagnetic radiation to the diffraction angle and the lattice spacing in a crystalline sample. These diffracted X-rays are then detected, processed and counted. A detector records and processes this X-ray signal and converts the signal to a count rate which is then output to a device such as a printer or computer monitor (Figure 2.4).

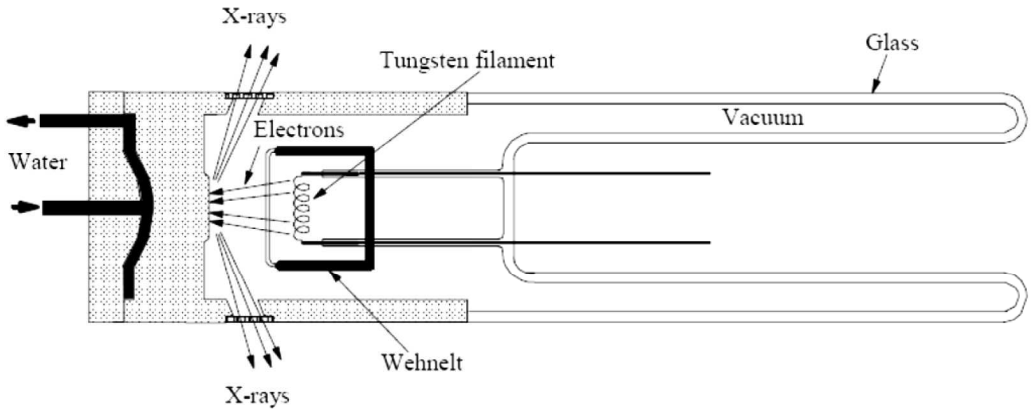

Figure 2.4 Diagram of X-ray generation.

In the XRD spectrometers two methods are applied for crystal structure determination.

1) Single Crystal XRD Method
2) Powder XRD Method

2.4.1 Single Crystal X-ray Diffraction (XRD) Method

Single crystal XRD is a non-destructive analytical technique which provides detailed information about the internal lattice of crystalline substances, including unit cell dimensions, bond-lengths, bond-angles, and details of site-ordering. Directly

related is single crystal refinement, where the data generated from the X-ray analysis is interpreted and refined to obtain the crystal structure.

Modern single crystal Diffractometer use CCD (charge-coupled device) technology to transform the X-ray photons into an electrical signal which are then sent to a computer for processing (Figure 2.5). We were used Bruker Smart and Oxford Diffractometer for the single crystal analysis.

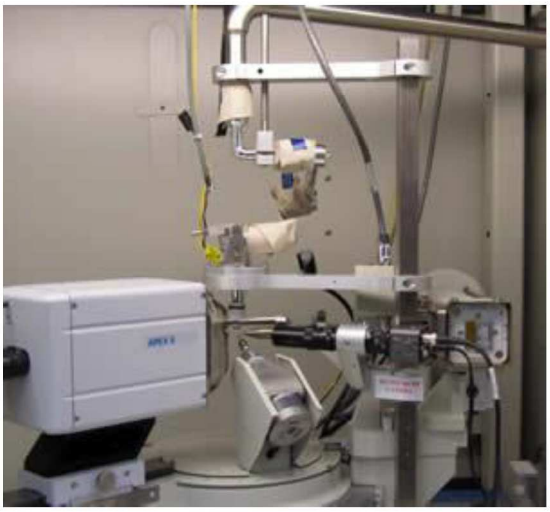

Figure 2.5 Single Crystal X-Ray Diffractometer, Bruker-Axis.

Single crystal XRD were performed on a Bruker Smart APEX II CCD area detector system equipped with a graphite monochromator and a Mo Kα fine-focus sealed tube operated at 1.5 kW power (50 kV, 30 mA). A crystal of compounds was adhered to a glass fiber using Paratone N oil. The detector was placed at a distance of 5.12 - 6.12 cm from the crystal during data collection. A series of narrow frames of data were collected with a scan width of 0.5º in ω or ϕ and an exposure time of 10 s per frame. The frames were integrated with the Bruker SAINT Software package using a narrow-frame integration algorithm. The data was corrected for absorption effects by the multi-scan method (SADABS). The structures were interpreted by the direct methods using the Bruker Apex2 Software Package. All non-hydrogen atoms were located in successive Fourier maps and refined anisotropically.

Single crystal XRD of compounds were measured on an Xcalibur Eos Oxford Diffractometer using graphite monochromator and a Mo Kα radiation (λ = 0.71073

Å). Absorption corrections were made using the multi-scan method. Data integration and reductions were processed with CRYS ALIS PRO software. Structure was analysed by the direct methods and then refined on F^2 using the full matrix least-squares technique with SHELX-97 software using the WINGX program package. All non-hydrogen atoms were located in successive Fourier maps and refined anisotropically. While hydrogen atoms were placed at the calculated positions using SHELX default parameters.

2.4.2 Powder X-ray Diffraction (XRD) Method

Powder XRD is a rapid analytical technique primarily used for phase identification of a crystalline material and can provide information on unit cell dimensions. The analyzed material is finely ground, homogenized, and average bulk composition is determined.

The geometry of an XRD is such that the sample rotates in the path of the collimated X-ray beam at an angle θ while the X-ray detector is mounted on an arm to collect the diffracted X-rays and rotates at an angle of 2θ. The instrument used to maintain the angle and rotate the sample is termed a goniometer. Conversion of the diffraction peaks to *d*-spacing allows identification of the mineral because each mineral has a set of unique *d*-spacing. Typically, this is achieved by comparison of *d*-spacing with standard reference patterns. For typical powder patterns, data is collected at 2θ from ~5 - 70°, angles that are preset in the X-ray scan (Figure 2.6).

Figure 2.6 Powder X-ray Diffractometer, D8 instrument.

For the powder XRD we were used Bruker D8 advanced instruments (Cu Kα radiation).

2.5 Thermal Analysis

Thermal analysis is the measurement of how specific physical or chemical properties of a substance changes with temperature. The early forms of thermal analysis were based mostly on Thermal Gravimetric Analysis where the change in weight of a substance with temperature was measured. The more important thermal analytical techniques are below

1) Thermo Gravimetric Analysis (TGA)
2) Differential Thermal Analysis (DTA)
3) Differential Scanning Calorimetry (DSC)
4) Thermo Magnetometry (TM)
5) Dielectric Thermal Analysis (DTA)
6) Differential Mechanical Thermal Analysis (DMTA)

We have used TGA, DTA and DSC technique for characterization among above mentioned most common thermal analysis techniques.

2.5.1 Thermo Gravimetric Analysis (TGA)

In this technique, the continuous weighting of a sample is monitored by a thermo balance as a function of temperature. The essential parts of thermo gravimetric instrument include; a container in the form of a crucible to hold the sample, a furnace that can heat the sample to a high temperature (HT), and an appropriate balance that can continuously monitor the sample. The sample container consists of a small platinum crucible suspended from the arm of a microbalance and situated in a small oven, the temperature of which is carefully monitored by a highly accurate thermocouple or some other appropriate temperature measuring sensor. For HT the platinum/30 % rhodium would be most common and would measure temperatures up to 1973 K. The balance is deflected as the sample weight changes as a result of temperature change and the consequent movement of the pan is sensed. The instrument normally gives an output in the form of a curve relating sample mass to

temperature but software is available to provide other forms of output, for example the differential form of the mass/temperature curve.

2.5.2 Differential Thermal Analysis (DTA)

The DTA measures temperature difference between a reference and sample as a function of time in a specified atmosphere. DTA is carried out by heating the sample together with a reference standard under identical thermal conditions in the same oven and measuring the temperature difference between the sample and reference substance during the period of heating. The reference standard must not suffer any change in state over the temperature range employed to examine the sample. As the temperature is increased any change in phase by the sample will result in a negative or positive temperature signal from the thermocouples. As soon as the sample changes state, crystal form, melts *etc*. the latent heat of phase transition will be absorbed and the temperature of the sample will lag behind that of the reference material. The temperature difference, ΔT, due to the phase transitions is detected by a thermocouple and converted to electrical signal, in μV, (Figure 2.7). DTA and DSC are very similar techniques but will be discussed separately.

Figure 2.7 TG/DTA, SII TG/DTA6300.

SII TG/DTA 6300 instrument were used for TG/DTA measurements. Measurements were carried out in the temperature range 300 K - 1025 K with heating rate of 10 K min^{-1} under nitrogen atmosphere by using. The compounds were transferred into a platinum pan and 4 - 20 mg compounds were used for each test. Total flow was maintained at 100 mL min^{-1} for TG/DTA measurement.

2.5.3 Differential scanning calorimetry (DSC)

DSC is a thermo analytical technique in which the difference in the amount of heat required to increase the temperature of a sample and reference are measured as a function of temperature. Whether more or less heat must flow to the sample depends on whether the process is exothermic or endothermic. For example, as a solid sample melts to a liquid it will require more heat flowing to the sample to increase its temperature at the same rate as the reference. This is due to the absorption of heat by the sample as it undergoes the endothermic phase transition from solid to liquid. Likewise, as the sample undergoes exothermic processes (such as crystallization) less heat is required to raise the sample temperature. By observing the difference in heat flow between the sample and reference, DSC is able to measure the amount of heat absorbed or released during such transitions. DSC may also be used to observe more subtle phase changes, such as glass transitions, study of oxidation, as well as other chemical reactions. DSC is widely used in industrial settings as a quality control instrument due to its applicability in evaluating sample purity and for studying polymer curing. The result of a DSC experiment is a heating or cooling curve. This curve can be used to calculate enthalpies of transitions. This is done by integrating the peak corresponding to a given transition (Figure 2.8). It can be shown that the enthalpy of transition can be expressed using the following equation:

$$\Delta H = K\mathrm{A}$$

Where, ΔH = enthalpy of transition, K = calorimetric constant and A = area under the curve.

Figure 2.8 DSC, Shimadzu DSC-60.

Shimadzu DSC-60 instrument was used for the DSC measurement. DSC measurements were performed in the temperature range 153 K - 453 K with the scanning rate 10 K min^{-1} under oxygen and nitrogen environments. 4 - 18 mg compounds were used for each test. The α-alumina material was used as reference for DSC. Total flow was maintained at 50 mL min^{-1} for DSC analyses.

2.6 Raman Spectroscopy

This technique is complementary to FT-IR and is a scattering technique, whereby a laser beam (near infrared region) is directed to the sample and the scattered radiation is collected. The applications are similar to FT-IR and gives useful information on the non-polar bonds, i.e. bonds with null or reduced dipole moment. Most of the scattered radiation has the same wave number as that of the incident laser beam; however a fraction will be having a different wave number. This is the Raman signal and characteristic of particular functional group.

The instrumentation comprises of exciting laser normally in near infrared region, Rayleigh filter, beam splitter, detector etc. The two types of laser source for Raman spectroscopy; the continuous wave source and the pulsed gas ion laser source. Raman spectrometers originally utilized continuous wave argon or krypton gas lasers. The gas used was important as the Raman scattering cross section varies as the fourth power of the light frequency. Thus, spectra obtained at 514.5 nm from an argon laser was from 2.3 to 4.5 times more intense than spectra obtained at 632.6 nm from a He-Ne laser operating at the same power. For additional power in the red region of the visible spectrum, dye lasers (pumped with a high power argon laser) were also employed to complement the basic gas lasers. Pulsed lasers in Raman spectrometers are not so common. The frequency doubled Nd/YAG laser with a fundamental at 1.06 mm was used because it was powerful, stable and reliable. Although it can be used in the continuous mode it was more often used in the pulsed mode with pulse widths of 10ns and a peak power output of 500 kW. Pulsed lasers were mostly employed for UV Raman analysis. Today diode lasers are commonly employed to produce excitation units in Raman spectroscopy and diode lasers having powers of 30 - 300 mW are readily available provide light at 785 nm and 830 nm. Tuneable lasers providing radiation between 670 - 1100 nm using Ti sapphire lasers are also readily

available. The great advantage of the diode laser is that it is monochromatic. The power used for the lasers, however, must be carefully controlled so as not to degrade the sample.

The collection system for the Raman scattered light comprises of two lenses the first a very short focal length with a low *f* number to collect the largest possible solid angle and the second focuses the collected light onto the entrance slit of a monochromator. Most instruments operate with a 90° or 180° scattering geometry. The 90° system is the easiest to operate as the since the illumination axis and the collection axis are apart in space. The 90° system can be modified to the 180° system by placing a small mirror prism on the face of the first lens (Figure 2.9).

Figure 2.9 Raman Spectrometer, HORIBA Jobin Yvon LabRAM-HR Spectrometer.

Raman spectra we were recorded with HORIBA Jobin Yvon LabRAM-HR Spectrometer using 488 nm excitation wavelengths from air cooled Argon ion laser for the region 100 - 1500 cm^{-1} and 633 nm excitation wavelengths from He-Ne laser for the region 2500 - 3700 cm^{-1} at a typical output power 5mw with a 50× objective.

2.7 Electron Paramagnetic Resonance (EPR)

The phenomenon of electron spin resonance (ESR), also called electron paramagnetic resonance (EPR), was discovered by the Soviet physicist Zavoisky in 1945, a year before the discovery of NMR by the American physicists Bloch and Purcell. Both NMR and EPR are collectively referred to as magnetic resonance

phenomenon. NMR and ESR are similar in their theoretical principles. However, while the former is observed in radiofrequency region and the later is observed in microwave region of the electromagnetic spectrum. ESR has limited applications because it is observed primarily in systems containing unpaired electrons. Thus, the systems which can be can be investigated by ESR spectroscopy are organic or inorganic free radicals and ions of transition metals which contain unpaired *d* or *f* electrons.

Every electron has a magnetic moment and spin quantum number $s = ½$, with magnetic components $m_s = +½$ and $m_s = -½$. In the presence of an external magnetic field with strength B_0, the electron's magnetic moment aligns itself either parallel ($m_s = -½$) or antiparallel ($m_s = +½$) to the field, each alignment having a specific energy. The parallel alignment corresponds to the lower energy state, and the separation between it and the upper state is $\Delta E = g_e \mu_B B_0$, where g_e = Lande *g*-factor, μ_B = Bohr magneton. This equation implies that the splitting of the energy levels is directly proportional to the magnetic field's strength, as shown below in the Figure 2.10.

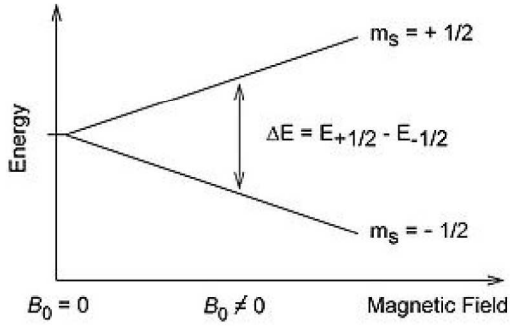

Figure 2.10 Diagram of energy level of an electron placed in magnetic field.

An unpaired electron can move between the two energy levels by either absorbing or emitting electromagnetic radiation of energy $\varepsilon = h\nu$ such that the resonance condition, $\varepsilon = \Delta E$, is obeyed. Substituting in $\varepsilon = h\nu$ and $\Delta E = g_e \mu_B B_0$ leads to the fundamental equation of EPR spectroscopy: $h\nu = g_e \mu_B B_0$. Experimentally, this equation permits a large combination of frequency and magnetic field values, but the great majority of EPR measurements are made with microwaves in the 9000 - 10000 MHz (9 - 10 GHz) region, with fields corresponding to about 3500 G (0.35 T). See below Figure 2.11, for other field-frequency combinations.

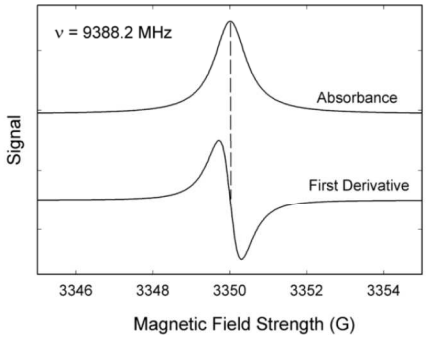

Figure 2.11 EPR spectrums as a function of strength, *B*, magnetic field.

In principle, EPR spectra can be generated by either varying the photon frequency incident on a sample while holding the magnetic field constant or doing the reverse. In practice, it is usually the frequency that is kept fixed. A collection of paramagnetic centres, such as free radicals, is exposed to microwaves at a fixed frequency. By increasing an external magnetic field, the gap between the m_s = +½ and m_s = -½ energy states is widened until it matches the energy of the microwaves, as represented by the double-arrow in the Figure 2.10. At this point the unpaired electrons can move between their two spin states. Since there typically are more electrons in the lower state, due to the Maxwell-Boltzmann distribution (Figure 2.11), there is a net absorption of energy, and it is this absorption that is monitored and converted into a spectrum.

The *g*-factor and the hyperfine coupling constant are the most important quantities determined from the ESR spectra of odd-electron systems. Thus, the ESR frequency of the odd electron is given by $v = g_e \mu_B B_0/h$, where h = plank's constant. Thus, the *g*-factor is essentially a measure of the ratio between frequency and magnetic field.

In the case of the transition metal ions and their complexes, there is considerable interaction between the spin and the orbital motion of the electron which prevents complete quenching of the orbital contribution. Hence, for such systems, the *g*-value departs from the g_e-value. In transition metal complexes containing *d* shells less than half-field, *g* is less than g_e while for shells more than half-field, *g* is greater than g_e. Also, the *g*-value is anisotropic, *i.e.*, its magnitude depends upon the direction of measurement. The anisotropy in *g*-value is shown the systems in the soled state where

conditions of restricted motion exist. In systems containing axial symmetry, the *g*-values along two dimensions, say, the *x* and *y* directions, are equal while the *g*-value along the *z* direction is different. If the magnetic field is applied along the *z* direction, the *g*-value is designated as $g_{\|}$ (*g* parallel). If the field is applied perpendicular to the *z*-axis (*i.e.*, if it is in the *xy* plane), the *g*-value is designated as $g_{\perp}$ (*g* perpendicular). In solutions, because of free rotating motion, the *g*-factor is isotropic *i.e.*, it is the average of the three *g*-values in the *x*, *y* and *z* directions.

We were used Bruker ESR spectrometer EMX at X-band frequencies with 100 KHz and 2 KHz modulation amplitude for temperature dependent EPR spectra.

2.8 Scanning Electron Microscope (SEM)

SEM is a type of electron microscope that images a sample by scanning it with a high-energy beam of electron in a raster scan pattern. The electrons interact with the atoms that make up the sample producing signals that contain information about the sample's surface topography, composition and other properties such as electrical conductivity.

In a typical SEM, an electron beam is thermionically emitted from an electron gun fitted with a tungsten filament cathode. Tungsten is normally used in thermionic electron guns because it has the highest melting point and lowest vapor pressure of all metals, thereby allowing it to be heated for electron emission, and because of its low cost. Other types of electron emitters include lanthanum hexaboride (LaB_6) cathodes, which can be used in a standard tungsten filament SEM if the vacuum system is upgraded and field emission guns (FEG), which may be of the cold cathode type using tungsten single crystal emitters or the thermally-assisted Schottky type, using emitters of zirconium oxide. The electron beam, which typically has an energy ranging from 0.5 - 40 keV, is focused by one or two condenser lenses to a spot about 0.4 - 5 nm in diameter. The beam passes through pairs of scanning coils or pairs of deflector plates in the electron column, typically in the final lens, which deflect the beam in the *x* and *y* axes so that it scans in a raster fashion over a rectangular area of the sample surface. When the primary electron beam interacts with the sample, the electrons lose energy by repeated random scattering and absorption within a teardrop-

shaped volume of the specimen known as the interaction volume, which extends from less than 100 nm to around 5 μm into the surface. The size of the interaction volume depends on the electron's landing energy, the atomic number of the specimen and the specimen's density. The energy exchange between the electron beam and the sample results in the reflection of high-energy electrons by elastic scattering, emission of secondary electrons by inelastic scattering and the emission of electromagnetic radiation, each of which can be detected by specialized detectors. The beam current absorbed by the specimen can also be detected and used to create images of the distribution of specimen current. Electronic amplifiers of various types are used to amplify the signals which are displayed as variations in brightness on a cathode tube. The raster scanning of the CRT display is synchronized with that of the beam on the specimen in the microscope, and the resulting image is therefore a distribution map of the intensity of the signal being emitted from the scanned area of the specimen. The image may be captured by photography from a high resolution cathode ray tube, but in modern machines is digitally captured and displayed on a computer monitor and saved to a computer's hard disk (Figure 2.12).

We were used JSM-5600, JEOL - Japan for the SEM analyses.

Figure 2.12 SEM, JEOL JSM-5600.

2.9 Mercury Porosimeter

Mercury porosimetry technique is one of the most useful methods to investigate the porous structure of solid samples in a quantitative way. It provides reliable information about pore size/volume distribution, bulk and apparent density and specific surface for most porous materials, regardless of their nature and shape. Mercury porosimetry analysis is based on the intrusion of mercury into the solid material porous structure under controlled pressurization. Mercury porosimetry analysis is based on the intrusion of mercury into the solid material porous structure under controlled pressurization. The pressurization procedure is critical to the accuracy and speed of the analysis because a certain equilibrium time is required for the mercury to fill pores at each pressure.

The Pressurization by Automatic Speed-up and Continuous Adjustment Logic (PASCAL), a new operating principle developed by the Microstructure department of Thermo Finnigan Italy and used in the new generation of automatic mercury porosimeter of the Pascal series. The PASCAL method automatically determines the correct pressurization speed according to the presence of pores and to the real penetration rate of mercury into the pores, thereby eliminating dead times during the analysis.

The pressurization starts 'softly' and, if no pores are detected, the speed of pressurization increases quickly to a maximum fixed speed. Nine speed characteristics are available covering different application fields and analytical purposes. When a speed from 1 to 9 is selected, the maximum speed is function of the actual pressure detected over the sample according to a matrix of values developed by the Microstructure staff; the higher is the pressure the higher is the maximum pressurization speed allowed. When the mercury begins to penetrate into the porous structure of the sample, the pressurization immediately slows down but without stopping completely. The acceleration and deceleration of the pumping system are properly balanced to assure exactly the correct equilibrium time for the complete penetration of mercury into pores showing the same access size. This method, therefore, allows to measured correctly the pore volume at the real penetration pressure, which is directly related to the pore size, while eliminating dead times.

Highest speed permits to collect a penetration curve up to 400 MPa in about 9 minutes. 'PASCAL' pressurization method eliminates the dead times automatically assuring equilibrium condition and does not require any prior knowledge about the sample characteristics (Figure 2.13).

For the mercury porosimetry analyses we were used Pascal 440, thermo - Italy.

Figure 2.13 Mercury Porosimeter, PASCAL 440.

2.10 Superconducting Quantum Interference Device (SQUID) Magnetometer

SQUID has been designed for magnetization measurements of small single crystals at low magnetic fields in the temperature range 2 K - 400 K. At LT the sensitivity in magnetic moments is 2×10^{-12} Am^2 or 2×10^{-9} emu, which is equivalent to $\Delta\chi = 10^{-7}$ SI with sample volume 3 mm^3 at 0.01 T (100 Oe).

The main part of SQUID magnetometer, i.e. SQUID unit, is shown in Figure 2.14. The unit is immersed in a He-bath at 2 K, and contains essentially the details: SQUID, a magnetic flux transformer including pick-up coils, magnet coil, heat switches and magnetic shielding.

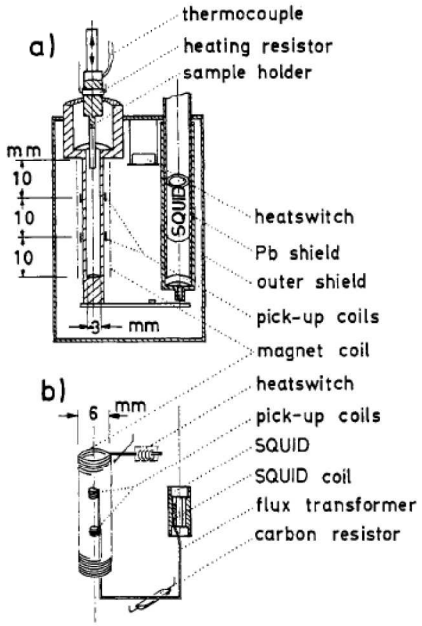

Figure 2.14 (a) Magnetometer unit, (b) Magnetic coil and flux transformer.

SQUID with its electronic circuits (from S.H.E. Manufacturing Corp, San Diego, California) can detect about 10^{-4} of a flux quantum ($\phi_0 = h/2e$). The magnetic flux transformer, made of superconducting Nb-wire (0.08 mm in diameter), consists of the pick-up coils, and SQUID coil. A satisfactory superconducting contact is achieved by pressing the wires mechanically together. During operation it is sometimes desirable to destroy the super current in the magnetic flux transformer. Thus a 10 kΩ carbon resistor is mounted in thermal contact with the wire. A carbon resistor was chosen rather than a heating coil in order to minimize unwanted magnetic fields near the magnetic-flux transformer. The magnetic-flux transformer has to be supported mechanically to avoid vibrations, and it must be rigorously shielded against external magnetic fields. The shielding is done by surrounding the twisted leads with superconducting lead. The whole SQUID unit is further enclosed in a superconducting lead can, and the cryostat is surrounded by three layers of μ-metal. The inner μ-metal can is immersed in liquid nitrogen in order to reduce fluctuations of the magnetic domains of the μ-metal.

The two counter wound pick-up coils have a diameter of 3.6 mm, each containing 30 turns. SQUID coil has 80 turns and a diameter of less than 2 mm, thus just fitting one of SQUID's holes. With this configuration 4.2 % of the flux change in a pick-up

coil is transformed into SQUID. The pick-up coils are wound on a copper cylinder, which separates the sample from the He-bath. The copper cylinder is attached to a stainless steel tube and forms a vacuum space for the sample. The sample may be heated by a small Allan-Bradley resistor attached to the sample holder (Figure 2.14), which is made of pure 99.999% copper. The temperature of this copper block is measured by copper-constantan, and gold (iron)-copper thermocouples attached to the upper part of the sample holder. The sample is glued to the lower part of the sample holder, which forms a 1.8 mm diameter copper pin of 18 mm length. (This arrangement is of great importance, since the heater and thermocouple otherwise might give rise to background noise in the transformer coil.) Because of the good thermal conductivity of copper, the temperature difference between the sample and the thermocouple never exceeds 0.5 K, even at 300 K.

The sample is magnetized by a superconducting magnet, operating in persistant mode. This mode of operation is essential, since a magnetic field of extreme stability is needed in order to avoid fluctuations caused by magnet current noise. The magnet coil produces a maximum field of 0.14 T, has a mean diameter of 6 mm, a length of 30 mm, and is made of 0.12 mm Nb-wire with 99.9% purity. Thus SQUID magnetometer works in a comparatively low region of magnetic field. Niobium was chosen as the material for both the superconducting magnet and the flux transformer circuit, since the intention has been to measure the magnetization at very low fields.

The magnetic field B is produced by the superconducting magnet coil. Then the sample is slowly moved through the pick-up coils. The magnetic moment of the sample induces a magnetic flux change in the pick-up coils. The magnetic flux transformer exhibits a superconducting loop, thus transforming part of the total magnetic flux change from the pick-up coils into SQUID. The pick-up coils are wound in opposite directions, thus compensating for external magnetic field variations. Highly magnetized samples must be moved very slowly through the pick-up coils in order not to exceed the maximum slewing rate of the electronic system. The sensitivity of magnetometers may be expressed in terms of the susceptibility χ. The magnetic moment of a sample is measured by passing it through the superconducting pick-up coil.

High field superconducting magnets must be supplied with a superconducting shield surrounding the pick-up coil and sample. In order to simplify the construction of the magnetometer pure copper was used as material for the support of pick-up coils and sample. Although this material is of very high purity, traces of iron or oxygen will introduce a temperature dependent paramagnetic signal. This is especially the case for the copper pin supporting the sample at very LT measurements. Copper further has a considerable nuclear paramagnetism, which also contributes to a temperature dependent background signal. The nuclear paramagnetism may be reduced by about two orders of magnitude by using silver or gold instead of copper. However, Johnson noise currents in metallic materials will give an extra contribution to signal noise. In order to eliminate the Johnson noise an insulator might be used. The pick-up coils could be wound on pure quartz, but the pin supporting the sample would have to be made of a material of good thermal conductivity, e.g. sapphire, crystalline quartz or silicon.

The magnetic measurements of our compounds were performed using a SQUID magnetometer in the temperature range of 2 K - 300 K. Variable temperature measurements were analyzed in the range of 2 K - 40 K. The ac-susceptibility measurements were carried out using a zero field.